An Integrated Machine Learning and Optimization Approach for Enhanced Strength Prediction in Riveted Joints

Kürşat Tanrıver[1] and Mustafa Ay[2]

[1]Faculty of Engineering and Natural Sciences, Department of mechatronics Engineering, Istanbul Health and Technology University, 34445 Beyoglu, Istanbul, Turkey

[2]Faculty of Technology, Department of mechanical Engineering, Marmara University, 34854 Istanbul, Turkey

e-mails: kursat.tanriver@istun.edu.tr;muay@marmara.edu.tr

Abstract: In this study, experimental tests, finite element analysis, and machine learning techniques were integrated to predict the maximum shear stress of riveted joints. First, ten tensile tests were conducted, yielding an average stress of 76.0383 MPa on the plates, and the regression analysis of the stress–strain data demonstrated a 95-99% level of agreement. A finite element analysis performed in Ansys under conditions similar to the experiments, produced a result of 78.875 MPa, which falls within an error margin consistent with the literature. Subsequently, a dataset of 20 samples containing various rivet diameters, plate thicknesses, hole coordinates and tensile loads was generated and used, to train a Regression Decision Tree model in MATLAB. For a new design case, the model predicted 7.480 MPa instead of 7.291 MPa, corresponding to an error of approximately 2.50%. When the dataset was expanded to 50 samples, this deviation decreased to 0.82%, indicating a significant improvement in accuracy. Overall, the results demonstrate that the machine learning model rapidly improves, as additional data become available and can provide reliable, fast predictions, including the effects of bending moments, offering a promising approach that may reduce the need for extensive experimental and numerical analyses.

Keywords: ANSYS; experimental work; Finite Element Analysis; Machine Learning; MATLAB; Riveted Joints

1 Introduction

Although rivets were initially used, followed by bolts, and later, welded joints were introduced to secure riveted connections [1], rivets continue to have a wide range of application today, due to their rigidity, reliability, difficulty in disassembly, high

strength, lightweight and cost-effectiveness, in industries such as aviation, automotive, shipbuilding, railway manufacturing and steel structures [2-4].

Various modeling methods have been developed in the literature to investigate the mechanical behavior of rivet and bolt joints. For instance, numerous experimental data have been obtained by conducting tensile tests on these joints [5]. Kang et al. [6] developed a series of mathematical models to examine the sequential deformation processes in aircraft panel riveting. These models provide a detailed analysis of the deformation behavior of riveted connections over time. Lu et al. [7] presented theoretical models of macroscopic and microscopic dynamics by examining connection structures in complex equipment. Seok and Kim [8] developed analytical models to simulate the cyclic behavior of cold-formed steel connections, particularly examining how local buckling effects influence the strength of connection elements. Zhou et al. [9] investigated the shear behavior of riveted rock joints, analyzing the factors affecting their behavior and proposing mathematical models.

Vrtač et al. [10] focused on evaluating the dynamic properties of riveted joints by indirectly assessing the rivet tightening force and determining joint impedances. The proposed method offers an approach particularly suitable for End-of-Line tests for riveted joints. Yang et al. [11] studied the strength properties of bonded, riveted and adhesive-rivet hybrid joints using Carbon Fiber Reinforced Plastic (CFRP). Finite element models of the composite joints were established and validated through quasi-static tensile tests. Wang et al. [12] worked on a new type of rivet joint for Cold-Formed Steel trusses. Parametric studies demonstrated that span-to-height ratio and lateral support positions significantly influence truss strength and failure modes. The results showed that the test-to-design strength ratio averaged 0.86, indicating that such connections can be evaluated in accordance with standards.

Tu et al. [13] developed a model aimed at optimizing riveted structures to address the stress concentration problem encountered in joining processes. The study examined how rivet cross-section shapes and ring groove sizes affect stress distribution. Several studies investigating stress values using software for algorithms and the Finite Element Method are as follows. Peng et al. [14] researched the development of high-strength Carbon Fiber Reinforced Polymer (CFRP) joints for rail vehicles. The study examined a hybrid joint system combining adhesive bonding and riveting techniques. Through finite element modeling and experimental testing, an optimized design strategy that improved load-carrying capacity by 27.9% was presented.

Arsadia [15] investigated the repeatability of bolt tightening under constant torque values using experimental data. Experiments were conducted on bolt-nut systems and examined under four different scenarios. Zabojszcza et al. [16] performed static strength analysis and optimization studies using the Monte Carlo Method on a simple bolted frame for building structures. Seitl et al. [17] investigated how crack

formation in rivet and bolt holes of steel bridges affects bridge strength. Qi et al. [18] created a model for connection plates on railway tracks. The finite element model of an angled guide plate was established to analyze the effects of bolt hole length, width, depth, and number on force distribution on the plate.

Grzywiński [19] coded the Jaya algorithm in MATLAB and compared results to find the minimum weight of tower structures. Dániel and Rad [20] built a full-scale experimental structure to examine the bending behavior of carbon fiber-reinforced polymer beams and conducted load tests. Serviceability limit states, standard loads, and load arrangements were examined during laboratory tests, and the experimental results were evaluated. Ibrahim et al. [21] investigated optimal elastic-plastic analysis methods for steel bars in reinforced concrete beams. ABAQUS was used for numerical experiments, and the concrete damage plasticity model was applied to represent concrete behavior. Tanrıver and Ay [22] proposed a method to investigate the effects of thermal expansion on rivet joints, using both MATLAB and Ansys software to estimate the resulting stress.

Keykha [23] examined the behavior and performance of reinforced steel by conducting finite element analysis using Ansys software. Ramasamy et al. [24] studied the design and mechanical behavior of two titanium-grade sheet metals. Forming force, sheet deformation, sheet thickness, and part profile accuracy were determined through experimental studies and finite element analysis.

In the literature review related to rivet and bolt joints, several studies employing machine learning are as follows. Sun et al. [25] developed a hybrid Deep Neural Network called SpatNet to improve the detection and quantification of rivet hole cracks in aviation environments. This approach shows significant potential for advancing intelligent ultrasonic testing. Lin et al. [26] predicted crack propagation in rivet holes on aircraft wings using a sample model. The study demonstrated that integrating machine learning methods with nominal stress analysis enhances prediction accuracy.

Kim and Youn [27] successfully detected cracks in riveted joints more accurately using the Physics-based Digital Twin Updating method. The study focuses specifically on machine learning-based crack detection and stress analysis. Hyung et al. [28] developed a hybrid model combining Gaussian Process Regression and the Enhanced Comprehensive Learning Particle Swarm Optimization algorithm to predict the ultimate strength of bolted steel connections. The model, validated with experimental data and finite element analysis, provided higher accuracy than existing machine learning models.

Kang et al. [29] integrated Acoustic Emission and Machine Learning algorithms to investigate the mechanical behavior and failure patterns of ultra-thin composite hybrid “bonded/bolted interference-fit” joints. The study analyzed damage categories using a structural damage index, improving accuracy and generalization ability through noise detection and isolation. This comprehensive review serves as a foundation for the research conducted in this paper.

The purpose of this study is to present a mathematical model for calculating the moments resulting from forces acting on connection plates, examining the model's impact on design, and investigating its industrial applicability. In the manuscript, a dataset consisting of maximum shear stresses was created based on different forces and variables using experimental and analytical methods on a sample model. Using this dataset, an innovative algorithm capable of predicting stress in other models not included in the dataset was developed. By filling a significant gap in literature, this algorithm can accurately calculate stresses occurring in bolted and riveted designs without the need for complex numerical methods, experimental setups, or finite element software. The proposed algorithm provides a practical, fast, and reliable method for researchers and practitioners.

2 Material and Method

For machine learning, the ANSYS program is frequently used for finite element analyses, while MATLAB is commonly employed for coding. The reliability of these tools is well-documented in the literature [30].

In this study, both experimental and theoretical-numerical methods were employed to determine the strength of riveted joints. In the initial phase, test specimens were prepared based on literature reviews and manufacturer data. To accurately reflect the moment effect observed in real-world applications, stress distributions were examined using finite element analysis (ANSYS) in addition to experimental tests.

Subsequently, the experimental data were compared with the finite element analysis results, and once it was confirmed that the error margin remained within the limits reported in the literature, further analyses were carried out using ANSYS models.

Initially, 20 different datasets containing maximum shear stress results were obtained using the structural analysis module. These datasets were then used to train a machine learning model (Regression Decision Tree) developed in the MATLAB environment.

Following this, a sample not included in the dataset was compared, using both the ANSYS simulation and the machine learning model. Afterward, an additional 30 datasets were generated, and the model’s performance was tested again on samples outside the dataset.

Thus, this work aims to develop a very accurate prediction approach for riveted joint strength.

2.1 Material

In this study, steel-riveted plates were used for the experiments. Considering real field conditions and the capacity of the testing device, a total of 10 test specimens

with the same type and properties were prepared [31] [32]. The prepared test specimens were designed to be compatible with the tensile testing device, with a width of 100 mm and a length of 150 mm.

For the specimens, 5 mm thick ST 37 plates were used, and steel rivets with a diameter of 4.8 mm and a length of 20 mm were employed for the connections. The plate surfaces were cleaned using the S_a 1 Light Blasting method according to the EN ISO 8501-1:2007 [30] standard, then primed and painted with black paint. The test specimens are shown in Figure 1, and the material properties are presented in Table 1 [33] [34].

Figure 1
Specimen [33]

Table 1
Material properties [34]

No	Description	Dimension	Piece	Material	Yield Strength (MPa)
1	Plate	5×100×150	2	ST 37	235
2	Rivet	4.8x20	2	Carbon Steel	160

2.2 Method

In this study, both experimental and numerical procedures were carried out in a structured manner to investigate the mechanical behavior of riveted joints. The methodology has been fully reorganized to provide clear, reproducible, and well-documented steps, covering the experimental setup, finite element modeling, and the development of the MATLAB-based machine learning model.

The materials used in the experiments consisted of ST37 steel plates with a thickness of 5 mm and carbon-steel rivets with a diameter of 4.8 mm. All plates were prepared following EN ISO 8501-1:2007 using Sa 1 Light Blasting, primed, coated, and left to dry for 24 hours to ensure consistent surface conditions. Handling procedures were standardized to avoid contamination.

Tensile tests were conducted using an Instron 5569 universal testing machine. The most used international standards for tensile testing of metal materials are ISO 6892-1:2016 and ASTM E8:2016 [33]. To comply with ISO 6892-1:2016, the environmental conditions were strictly controlled at 23 ±2°C and 45-55% relative humidity, and the strain rate was set to 2 mm/min (Method A). Prior to testing, the machine calibration was performed in accordance with manufacturer guidelines. Each specimen was aligned through a centering fixture, and the gripping rods welded to the plates ensured consistent loading and prevented slippage. The tensile load was applied until complete shear failure of the rivets, and force–displacement data were recorded at 10 Hz.

Finite element models can be used to validate the suitability of these methods by examining the static behavior of connection elements [28] [35]. Among the software tools utilizing these methods, the ANSYS program enables the numerical analysis of shell elements in terms of buckling and shear loads [36]. This allows experimental investigations to be examined in a numerical context. Studies examining experimental tests and numerical simulation approaches for blind rivet connections are also available [37].

The numerical analysis was performed using Ansys R19.2 academical. A full 3D solid model of the riveted joint was created using Solidworks academical version elements. Contact interactions were defined using hard normal contact and penalty friction ($\mu = 0.25$), and the boundary conditions were applied to reflect real-world eccentric loading that induces bending moments. The model consisted of 8189 elements and 41453 nodes.

To enhance transparency and numerical reliability, a mesh convergence study was performed using 5 mm, 3 mm, and 2 mm mesh sizes. The difference in maximum shear stress between the 3 mm and 2 mm meshes remained below 2%, confirming that the simulation results had reached mesh-independent (converged) values. Therefore, all FEM simulations were executed using a 3 mm Sweep Mesh, which provided an optimal balance of computational efficiency and accuracy.

Furthermore, a sensitivity analysis involving variations in friction coefficient (μ = 0.15-0.35), applied load (±10%), and boundary stiffness (±20%) demonstrated that the maximum shear stress changed by less than 3.1%, indicating that the numerical model is stable and robust under perturbations in key parameters.

A parametric finite element model was used to generate datasets representing different rivet diameters, plate thicknesses, hole coordinates, and tensile loads. Initially, 20 samples were generated and later expanded to 50, to improve predictive performance.

Machine learning analysis was carried out using MATLAB's Regression Decision Tree function (fitrtree). The dataset was divided using an 80/20 train-test split, and a fixed random seed (42) was used for reproducibility. Model performance was evaluated using MSE, RMSE, and R^2 metrics. Two unseen configurations were used

to compare MATLAB predictions with ANSYS results, yielding deviations of 2.50% (20 samples) and 0.82% (50 samples), respectively.

Through these revisions, the methodology now provides a complete, step-by-step description of experimental, numerical, and computational procedures, ensuring that the study can be fully reproduced by other researchers.

3 Results and Discussion

3.1 Tensile Test

Tensile strength tests were conducted to investigate the tensile performance of rivets. Additionally, there are studies that analyze the tensile process using the finite element method, compare the results with test data, and achieve significant compatibility [28].

Before starting the stress analysis, it is necessary to examine the loads applied to the connecting elements. Tensile tests were applied individually to the rivet-connected test specimens. Although the test specimens were geometrically identical prior to the tensile tests, differences were observed in their behavior.

Some specimens exhibited significant elongation and fracture under low tensile forces, while others displayed noticeable bending. A summary of the test results is presented in Table 2.

Table 2
Tensile test result summary

Rivet Diameter	Plate Dimensions	Specimen Name	Tensile stress (MPa)
4.80	5×100×150	Specimen 1	73.962
4.80	5×100×150	Specimen 2	56.589
4.80	5×100×150	Specimen 3	81.501
4.80	5×100×150	Specimen 4	55.291
4.80	5×100×150	Specimen 5	92.851
4.80	5×100×150	Specimen 6	82.765
4.80	5×100×150	Specimen 7	79.213
4.80	5×100×150	Specimen 8	78.582
4.80	5×100×150	Specimen 9	71.465
4.80	5×100×150	Specimen 10	88.164

The average of the results is found to be 76.0383 MPa, and this value is planned to be used in all calculations. Before the experiments, the calibration of the testing device was completed, and during the experiments, the device's settings and control mechanisms were meticulously examined to prevent potential errors.

Additionally, regression analysis was performed to evaluate unexpected stress distributions and factors that could influence the results during the experiments.

The analysis was conducted by considering the data up to the maximum stress level that a single rivet could withstand before failure. The regression analysis curve demonstrated a high level of compatibility between the Tensile Stress - Tensile Strain values obtained from the experiment.

The compatibility ratios were determined as 97.20%, 99.30%, 99.60%, 95.80%, 99.50%, 98.91%, 98.70%, 98.66%, 98.25% and 99.23%, respectively. These values indicate that the Tensile Stress - Tensile Strain values are consistent with each other at the specified levels.

3.2 Finite Element Analysis

In traditional rivet stress calculations, the shear force is applied by dividing it by the cross-sectional area of the rivet. However, considering the existing studies and the experiments conducted on rivets, it has been observed that the plates carrying the rivets are mostly subjected to oblique tensile loading.

This indicates that the rivets are exposed not only to shear force but also to a bending moment. Since this situation is expected to cause a discrepancy between the finite element analysis and laboratory experiments, finite element analysis was conducted after performing these calculations.

When a tensile load is applied to the plates, it is assumed that this load generates stress within the plane of the tensile axis [38], and calculations are made based on this assumption. However, it is well-known, that this is not entirely accurate in tensile tests and real loading conditions [39].

Due to the off-center application of the tensile load, the plates are forced to bend, resulting in the formation of a moment. A literature review has revealed studies pointing to the improvement of connector geometry and the formation of moments when loads are applied eccentrically [40-43]. However, no study has been found that explains or formulates these findings with additional equations.

Additionally, there are studies suggesting that the load applied to the connectors is not necessarily proportional to the number of connectors. These studies modeled the load on the connectors and compared the results with experimental data [44]. It should be emphasized that this situation arises from the inability to apply purely axial tensile force.

When calculating the shear load on the bolts, including the stresses caused by this moment in the calculations provide more accurate results. The bending moment occurs at a certain angle within the cross-sectional plane. The plate model under moment loading is shown in Figure 2.

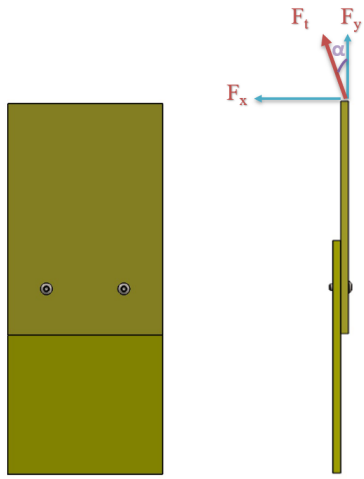

Figure 2
The specimen model under tensile testing

When the angle in the direction of the tensile force is denoted as α, two forces are generated on the plates: one horizontal (F_x) and one vertical (F_y). The moments produced by these two forces lie in the same plane, but their directions are opposite to each other.

The angle α formed within the cross-sectional plane, as well as the vertical force F_y and the horizontal force F_x, are expressed by the following equations:

$$\alpha = tan^{-1}\, l_2 \,/l_1 \tag{1}$$

$$F_x = F_t \sin\alpha \tag{2}$$

$$F_y = F_t \cos\alpha \tag{3}$$

The rivet moments Mx and M_y are given by the equations below: the distance of F_y to the pivot point is l_1, the distance of F_x to the pivot point is l_2, the vertical force is F_y, and the horizontal force created by these forces is F_x.

$$M_x = F_x\, l_1 \tag{4}$$

$$M_y = F_y\, l_2 \tag{5}$$

$$M_{net} = M_y - M_x \tag{6}$$

Here, F = 2670.10 N, F_x = 159.74 N, F_y = 2665.31 N, l_1 = 150 mm, l_2 = 7 mm, M_x = 23961 N.mm, M_y = 18657.17 N and M_{net} = 5303 N.mm

The moment of inertia I in the moment direction, the plate thickness h, the plate width g, and the tensile-compression stress $S_{t/c}$ due to Mnet are given below.

$$I = h\, g^3 \,/12 \tag{7}$$

$$S_{t/c} = M_{net}\, y_{max} \;/I \tag{8}$$

Here, as h =5 mm, g = 100 mm, the moment of inertia of the plate in the moment direction is calculated as I=1041.67 mm^4, y_{max} = 2.5 mm and $S_{t/c}$ = 12.73 MPa.

Considering the bending moment occurring in the plates and the resulting neutral axis, tensile-compressive stress is generated within the plate. As a result of this tensile-compressive stress, an additional virtual shear force acting in the opposite direction of the rivet will be produced.

It is observed that the sum of this virtual shear force and the shear forces generated in the plate during tensile loading is equal to the actual active shear stress that breaks the rivets. To calculate this virtual shear force, it is necessary to determine the surface area of the rivet related to the crushing region, rather than the shear area.

Thus, the complex stress state occurring in the rivet joint can be modeled more accurately.

The crush area A_{cr} and the virtual shear force F_{im} are shown by the following equation:

$$A_{cr} = h\, D_{riv} \tag{9}$$

$$F_{im} = S_{t/c}\; A_{cr} \tag{10}$$

Here, H = 5 mm, D_{riv} = 4.80 mm, and $S_{t/c}$ = 12.73 MPa, A_{cr} = 24 mm^2 and F_{im} = 305.52 N

The virtual force is found to be F_{im}=305.52 N, which corresponds to 1.14% of the force applied to the plate, F_t=2670.10 N. This ratio is significant enough to be considered and cannot be neglected.

In this case, the total shear force acting vertically on the experimental plate under real conditions can be determined by adding these two forces. The equation is shown below.

$$F_{sh} = F_y + F_{im} \tag{11}$$

Here, since Fy=2665.31N and F_{im}= 305.52 N, the total shear force is calculated as F_{sh}=2970.50 N. Additionally, it was previously found that F_x=159.74 N.

As can be seen, the test plates in the real case are not only subjected to the tensile force F_T=2670.10 but also experience additional forces due to the moment effect. The studies reveal that the test plates are actually exposed to a vertical shear force of 2970.50 N and a horizontal force of 159.74 N.

Since this situation creates similar conditions to real field scenarios, it is recommended that readers and designers take this aspect into account.

The forces obtained from experimental tests and calculations were utilized for finite element analysis performed using the ANSYS R19.2 program, as well as for

analytical calculations to carry out the intended studies. The force definition is presented in Figure 3.a.

The contact between the plates was defined as surface-to-surface contact. Similarly, the connection between the plate and the rivet was also specified as surface-to-surface contact. Furthermore, for surface-to-surface contact, the tangential behavior was defined as penalty friction, and the normal behavior was defined as hard contact.

The analysis employed a total of 8189 finite elements and 41453 nodes. The mesh size was determined as 3 mm using the Sweep Meshing technique. The mesh analysis is described in Figure 3.b. Subsequently, the problem was solved using the Maximum Shear Stress criterion. The finite element model is shown in Figure 3.c.

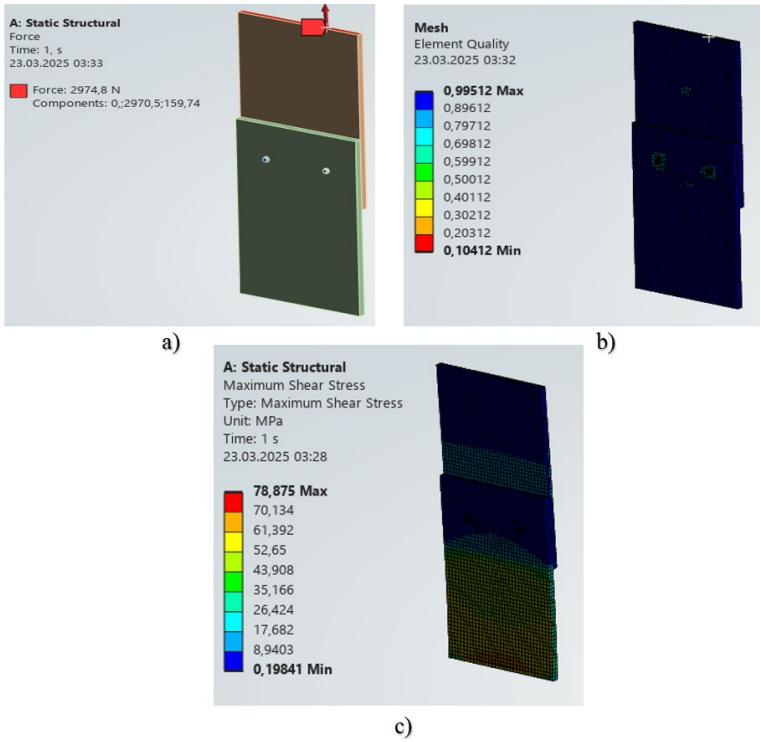

Figure 3
Maximum shear analysis

Analysis Result a) Force- Boundary Conditions b) Mesh Element Quality c) Maximum Shear Stress

As a result, the maximum shear stress obtained from the finite element analysis was found to be 78.875 MPa. The ratio between the finite element analysis result and the average experimental result from Table 2 (76.0383 MPa) was determined to be 1.037.

Similarly, when examining studies in literature, it is observed that ratios between experimental results and finite element analysis results are reported. For instance, Guo et al. [31] found this ratio to be 1.77, Tanriver and Ay [38] reported it as 1.003, and Nguyen et al. [39] obtained a ratio of 1.02. The value obtained in this study falls within the range of values observed in the existing literature.

3.3 Modelling and Data set for Machine Learning

3.3.1 Modelling

After confirming the reliability of the finite element analysis with a ratio of 1.037 compared to the literature, it was decided to generate data for machine learning. For this purpose, a model was created in the Ansys Static Structural module to perform maximum shear analysis on a design subjected to loading without generating a moment in a flat configuration.

To determine the Max. Shear Stress result, a model was constructed by joining two plates of dimensions 2x1150x300 with four rivets of 2.40 mm. The model details are presented in Table 3, and the model design is illustrated in Figure 4.

Table 3
Model Design Information

No	Plate Thickness	Rivet diameter	x_1	y_1	x_2	y_2	x_3	y_3	x_4	y_4	F_t	Max. Shear Stress
1	2	2.4	60	75	120	75	180	75	240	75	3200	

Thus, a machine learning model was designed to predict the maximum shear stress value of riveted joints using this model. The dataset was generated from ANSYS simulation results, which were validated by comparison with both experimental results and literature.

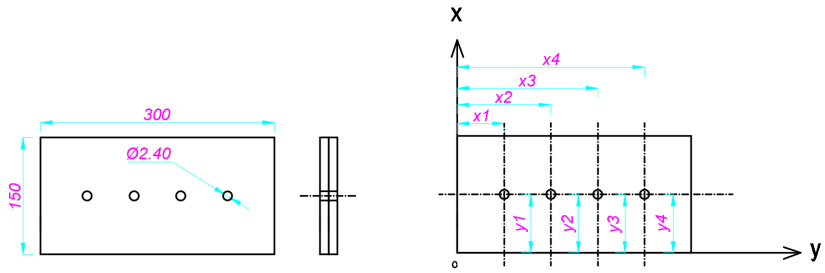

Figure 4
Model Design Information

Here, PlateThickness represents the plate thickness (mm), RivetDiameter denotes the rivet diameter (mm), and x_1, y_1, x_2, y_2, x_3, y_3, x_4, $_y4$ indicate the rivet coordinates

(mm). F_t refers to the applied tensile force (N), while Max Shear Stress is the target variable measured in ANSYS (MPa).

The flowchart shown in Figure 5 illustrates the step-by-step prediction process of riveted joint shear stress using machine learning. The process begins with data collection for riveted joint stress analysis (Step 1), followed by feature-target selection (Step 2) and splitting the data into training and testing sets (Step 3). Next, a decision tree model is trained (Step 4) and evaluated (Step 5). If the performance is satisfactory, new data can be predicted (Step 6). Otherwise, hyperparameter tuning or additional data collection is required to improve the model.

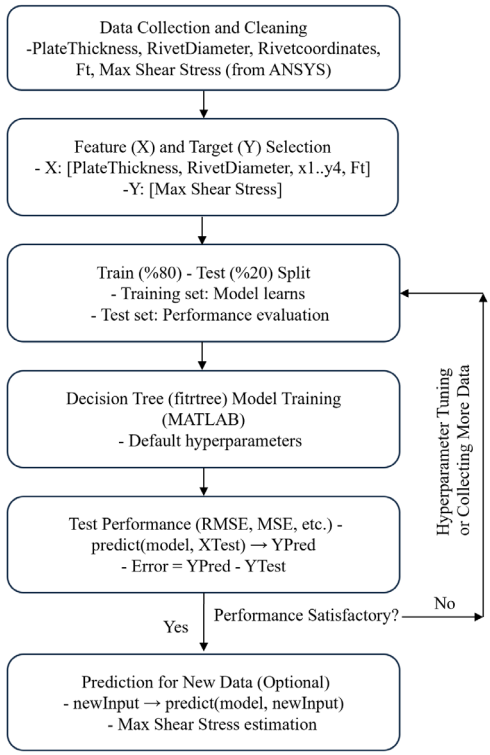

Figure 5
Machine learning flowchart for rivet joint stress analysis

As shown in the flowchart, a table containing the ANSYS results is first created. Then, the model training and testing performance are measured. Finally, a new configuration not included in the table is entered to quickly predict the “Max Shear Stress” value.

The dataset is planned to include 20 rows of sample input data, with 80% allocated for training and 20% for testing. The model will utilize MATLAB's Regression Decision Tree function (fitrtree). The model's accuracy will be assessed using

performance metrics such as Mean Squared Error (MSE), Root Mean Squared Error (RMSE), and R^2 to evaluate its effectiveness.

3.3.2 Generating a Data Set and Predicting Results

The model was assigned a 4 mm mesh sizing and a 2 mm resolution mesh. A total of 46648 nodes and 8451 elements were defined for this model. To define the boundary conditions, fixed support was applied, and a tensile force of 3200 N was introduced. The mesh element quality analysis of the model is shown in Figure 6.a, while the boundary conditions are illustrated in Figure 6.b.

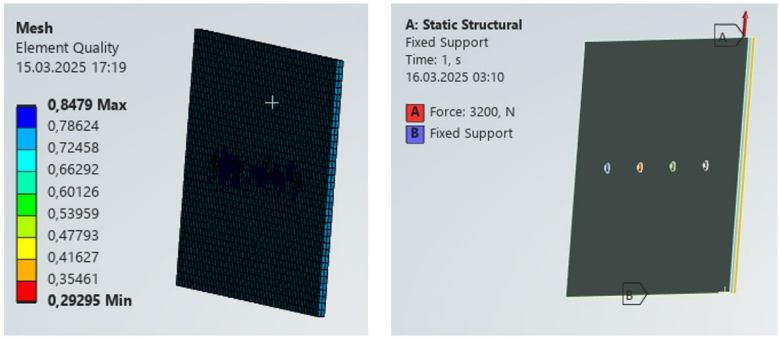

Figure 6

Design specifications a) Element Quality b) Boundary conditions

Subsequently, total deformation and maximum shear stress analyses were performed on the model. The results of these analyses are presented in Figure 7.

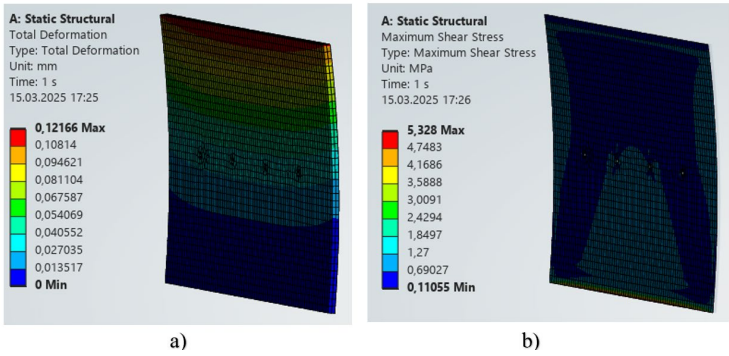

Figure 7

Analysis Result a) Total Deformation b) Maximum Shear Stress

According to the analysis, the maximum total deformation was found to be 0.12166 mm, and the maximum shear stress was calculated as 5.3280 MPa. Therefore, it was planned to create a dataset for machine learning. Based on the model described

above, 20 maximum shear stress analyses were performed by varying plate thicknesses, rivet diameters, rivet positions, and tensile loads while keeping the plate width and length constant. The results are presented in Table 4.

Table 4
Data set

No	Plate Thickness	Rivet diameter	x_1	y_1	x_2	y_2	x_3	y_3	x_4	y_4	F_t	Max. Shear Stress
1	2	2.4	60	75	120	75	180	75	240	75	3200	5.3280
2	3	3.0	26	117	107	132	172	121	234	126	3600	8.8126
3	4	2.4	98	98	124	124	140	140	211	127	2750	5.5570
4	5	3.0	60	115	86	80	160	75	201	136	1800	3.9753
5	2	2.4	53	100	99	121	174	104	205	92	2400	7.1840
6	4	4.80	20	50	89	118	210	131	283	62	3400	10.9380
7	5	6.00	59	45	87	50	180	134	258	88	2100	4.6448
8	2	6.00	100	123	119	134	215	113	256	115	800	2.5762
9	3	2.40	39	30	108	126	161	135	241	136	1500	3.6723
10	4	3.00	36	120	132	75	198	115	270	40	1250	2.5275
11	5	2.40	52	124	85	122	165	23	220	28	1250	2.7510
12	5	4.00	52	75	107	85	157	65	244	71	1100	2.4202
13	1	2.40	54	129	106	122	150	116	204	105	750	4.1032
14	5	4.00	61	24	120	35	183	119	285	122	1580	3.4891
15	3	2.40	34	133	103	127	189	126	275	130	2400	5.8800
16	1	4.80	28	122	105	124	150	134	240	130	980	5.2580
17	2	6.00	52	117	94	123	169	119	244	131	2650	8.5394
18	3	6.00	37	117	113	130	159	120	237	91	3100	7.6012
19	4	2.40	58	132	114	129	165	134	230	131	1600	3.2328
20	1	4.00	51	60	113	65	153	75	217	80	500	2.6759

After training the initial dataset of 20 entries in the machine learning model in MATLAB, a new model, which was not part of the original dataset, was analyzed using finite element analysis in the ANSYS program. Then, the results were

predicted using the machine learning model in MATLAB. The ANSYS Maximum Shear Stress analysis results are shown in Figure 8.a, and the MATLAB model prediction results are displayed in Figure 8.b.

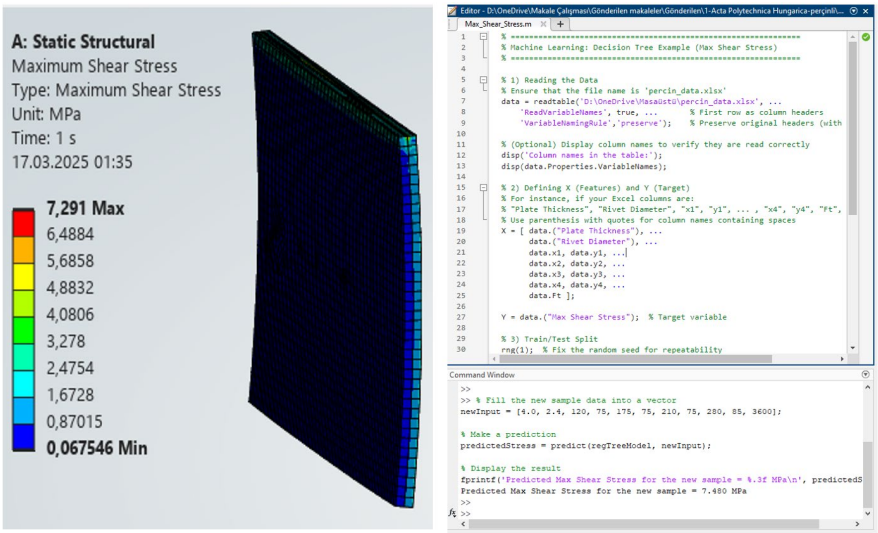

a) b)

Figure 8

Maximum Shear Analysis Result for first 20 Data

a) Finite Element (Ansys) b) Prediction of result (MATLAB-Machine Learning)

According to the results, the Maximum Shear Stress value obtained from the ANSYS program for the new model is 7.291 MPa. The machine learning prediction in MATLAB estimated the value to be approximately 7.480 MPa. The difference between these two results is 0.189 MPa, indicating a deviation of 2.5%. This deviation is found to be consistent with the literature [45] [46].

To enhance the model's capability and prediction accuracy, an additional 30 maximum shear stress analyses were performed by varying plate thicknesses, rivet diameters, rivet positions, and tensile loads. The expanded dataset, which includes the new inputs and results prepared in ANSYS, is presented in Table 5.

Table5
Data set

No	Plate Thickness	Rivet diameter	x_1	y_1	x_2	y_2	x_3	y_3	x_4	y_4	F_t	Max. Shear Stress
21	5	2.40	52	124	85	122	165	23	220	28	3500	7.7000
22	5	4.00	52	75	107	85	157	65	244	71	3500	7.6997
23	1	2.40	54	129	106	122	150	116	204	105	3500	25.3490
24	5	4.00	61	24	120	35	183	119	285	122	3500	7.7000
25	3	2.40	34	133	103	127	189	126	275	130	3500	8.5763
26	2	2.4	60	75	120	75	180	75	240	75	2000	3.3310
27	3	3.0	26	117	107	132	172	121	234	126	4500	11.016
28	4	2.4	98	98	124	124	140	140	211	127	3500	7.0725
29	5	3.0	60	115	86	80	160	75	201	136	1000	2.1982
30	2	2.4	53	100	99	121	174	104	205	92	4000	12.6840
31	5	2.40	52	124	85	122	165	23	220	28	4000	8.8004
32	5	4.00	52	75	107	85	157	65	244	71	3000	6.5991
33	1	2.40	54	129	106	122	150	116	204	105	4000	28.8360
34	5	4.00	61	24	120	35	183	119	285	122	2250	4.9605
35	3	2.40	34	133	103	127	189	126	275	130	6000	14,70
36	4	4.80	20	50	89	118	210	131	283	62	10000	32.1630
37	5	6.00	59	45	87	50	180	134	258	88	5000	11.0320
38	2	6.00	100	123	119	134	215	113	256	115	5000	18.5850
39	3	2.40	39	30	108	126	161	135	241	136	3000	7.3439
40	4	3.00	36	120	132	75	198	115	270	40	5000	10.1090

No	Plate Thickness	Rivet diameter	x_1	y_1	x_2	y_2	x_3	y_3	x_4	y_4	F_t	Max. Shear Stress
41	2	2.4	60	75	120	75	180	75	240	75	4000	6.6620
42	3	3.0	26	117	107	132	172	121	234	126	4400	10.771
43	4	2.4	98	98	124	124	140	140	211	127	3550	7.1736
44	5	3.0	60	115	86	80	160	75	201	136	2600	5.7155
45	2	2.4	53	100	99	121	174	104	205	92	3200	10.2910
46	4	4.80	20	50	89	118	210	131	283	62	4000	12.8660
47	5	6.00	59	45	87	50	180	134	258	88	3000	6.6201
48	2	6.00	100	123	119	134	215	113	256	115	1500	5.5755
49	3	2.40	39	30	108	126	161	135	241	136	2000	4.8959
50	4	3.00	36	120	132	75	198	115	270	40	1800	3.6392

In the MATLAB program, the machine learning model was trained with a total dataset of 50 entries. Subsequently, a new model, which was not part of the dataset, was analyzed using finite element analysis in the ANSYS program. The results were then predicted using the machine learning model in MATLAB. The ANSYS Maximum Shear Stress analysis results are displayed in Figure 9.a, while the MATLAB model prediction results are shown in Figure 9.b.

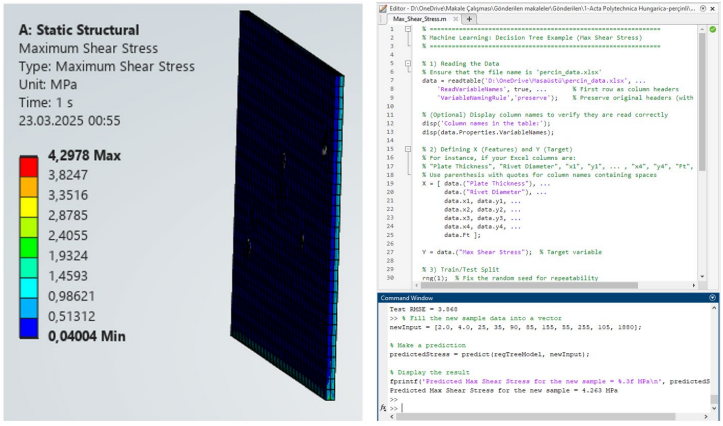

a) b)

Figure 9

Maximum Shear Analysis Result for 50 Data

a) Finite Element (Ansys) b) Prediction of result (MATLAB-Machine Learning)

For the model trained with a dataset of 50 entries, the Maximum Shear Stress value for a sample not included in the dataset was found to be 4.2981 MPa using the ANSYS program. The machine learning prediction in MATLAB estimated this value to be approximately 4.263 MPa. The difference between these two results was calculated as 0.0351 MPa, resulting in a deviation of 0.82%. This deviation is consistent with the literature [45] [46].

Thus, it is evident that when the dataset is increased from 20 to 50 entries, the prediction accuracy improves significantly.

3.4 Error Analysis

An error analysis is necessary to enhance the understanding of the studies presented in this manuscript. The error rates can be determined using the following equations.

$$\text{Total Error } (\%) = \frac{\text{Targeted result-Calculated result}}{\text{Targeted result}} \tag{12}$$

Based on this equation, an error analysis was conducted to evaluate the uncertainties in the experimental and simulation results. According to the analysis, the comparison of simulation results with experimental data and a summary of the total error rate are presented in Table 6.

Table 6
Total Error

No	Parameter	Targeted Result (MPa)	Calculated Result (MPa)	Total Error (%)
1	Experimental Result- Finite Element Result (Ansys)	76.0383	78.875	-3.73
2	Finite Element Result (Ansys) - Prediction of result (MATLAB-Machine Learning) for First 20 Data Set	7.291	7.48	-2.59
3	Finite Element Result (Ansys) - Prediction of result (MATLAB-Machine Learning) for 50 Data Set	4.2981	4.263	0.82

When the results listed as number 1 in the table are compared with the literature [31, 38, 39], they are found to be consistent. Similarly, the results listed as numbers 2 and 3 are in agreement with the literature [45] [46].

Conclusions

In this study, a comprehensive investigation was conducted by integrating experimental analysis, finite element analysis and machine learning methodologies to predict the maximum shear stress in riveted joints. Initially, tensile tests were performed on 10 specimens, and the average stress obtained from these samples was measured as 76.0383 MPa. To evaluate the compatibility of the experimental results, regression analysis was conducted, revealing correlations of 97.20%,

99.30%, 99.60%, 95.80%, 99.50%, 98.91%, 98.70%, 98.66%, 98.25% and 99.23%, between tensile stress and tensile elongation values, respectively.

Taking into account the effects encountered under real field conditions and during tensile testing, the forces applied to the plates were calculated mathematically. The findings indicate that the test plates are subjected not only to the 2670.10 N force from the experimental setup but also to a vertical shear force of 2970.50 N and a horizontal force of 159.74 N. These results demonstrate that the plates are exposed to not only tensile force but also moment effects arising from eccentric loading.

Considering these calculated forces, the Maximum Shear Stress obtained from the Finite Element Analysis conducted using the Ansys R19.2 Structural Analysis module was found to be 78.875 MPa. The ratio between the experimental average result (76.0383 MPa) and the FEA result was determined to be 1.037, which is considered acceptable, according to studies in the literature.

After confirming that the finite element method is at an acceptable level, shear stress analysis was performed using the Ansys structural analysis module to generate datasets. In this context, a dataset consisting of 20 samples was created by considering different rivet diameters, plate thicknesses, hole coordinates, and tensile loads. This dataset was then used as input for a Regression Decision Tree (fitrtree) model trained in the MATLAB environment. When the model was presented with a design that it had not previously seen, the maximum shear stress obtained from the Ansys analysis was 7.291 MPa, while the machine learning model predicted a maximum shear stress of 7.480 MPa and a deviation of 2.50%.

Furthermore, to enhance the model's accuracy, the dataset was expanded by adding 30 additional samples, bringing the total to 50 samples. Similarly, for a new design, the maximum shear stress obtained from the Ansys analysis was 4.2981 MPa, while the machine learning model predicted a maximum shear stress of 4.263 MPa. This corresponds to an error margin of only 0.82%. When all findings are evaluated:

- As the number of data points increases, the generalization capability and accuracy of the machine learning model significantly improve.
- The error between the experimental results and the Ansys analysis is within the acceptable range established in the literature.
- While the machine learning model initially exhibited a deviation of 2.50%, this deviation was reduced to 0.82% with the addition of more data.
- Thus, maximum shear stress prediction can be easily achieved using a machine learning algorithm in the riveted plate model without relying on experimental methods or finite element analysis.
- This approach is expected to provide designers with a significant speed advantage by eliminating the need for time-consuming and complex studies.

The approach presented in this study offers both fast and highly accurate predictive capabilities. Unlike traditional methods based solely on classical shear approaches, this methodology takes into account details such as moment effects, leading to more reliable and realistic results in the design of riveted joints. This approach can be further improved by using larger datasets or different machine learning algorithms for future studies and can be effectively applied in both academic research and industrial applications.

In future studies, the numerical and experimental framework will be expanded to incorporate material anisotropy, geometric nonlinearity and fatigue behavior, which can significantly influence the reliability of riveted joints under real operating conditions. Advanced material models such as elastic plastic or orthotropic formulations along with a more detailed representation of local plastic deformation and contact interactions around the rivet zone will be implemented to improve the accuracy of the finite element analysis.

Additionally, long-term experimental investigations considering various loading scenarios, repeated impact effects, and environmental factors (temperature, humidity, corrosion) are planned to evaluate their influence on joint integrity. The insights gained from these extended analyses are expected to enhance model fidelity and support the development of more robust and durable riveted joint designs.

Acknowledgement

This research did not receive any specific grant from funding agencies in the public, commercial, or not-for-profit sectors.

References

[1] Wu, J., Chen, C., Ouyang, Y., Recent development of the novel riveting processes, International Journal of Advanced Manufacturing Technology, 117 (2021) 19-47, https://doi.org/10.1007/s00170-021-07689-w

[2] Beber, M., Stejskal, M., Sedlacek, F., Determination of Mechanical Properties of Blind Rivet Joints Using Numerical Simulations and Experimental Testing, Materials, 18 (2025) 229, https://doi.org/10.3390/ma18020229

[3] Unterweger, H., Derler, C., Fatigue tests and calibrated fracture mechanics approach for historical riveted steel girders, Journal of Constructional Steel Research, 176 (2021) 1-21

[4] Tanriver, K., Ay, M., Experimental, Software and Topological Optimization Study of Unpredictable Forces in Bolted Connections, Tehnički vjesnik, 30 (2023) 1175-1184, https://doi.org/10.17559/TV-20221113121639

[5] Sire, S., Mayorga, L. G., Plu, B., Observation of failure scenarios in riveted assemblies: an innovative, 1st International Conference on Structural Integrity, France, 2015

[6] Kang, Y., Song, S., Wang, T., Li, G., Wang, Z., Chen, Y., Study on the Mechanism of Cumulative Deformation and Method for Suppression in Aircraft Panel Riveting, Aerospace, 11 (2024) 678, https://doi.org/10.3390/aerospace11080678

[7] Lu, X., Zhu, M., Wang, S., Li, S., Xu, Z., Liu, Y., Progress in Theoretical Modelling of Macroscopic and Microscopic Dynamics of Bolted Joints in Complex Equipment, Lubricants, 12 (2024) 182, https://doi.org/10.3390/lubricants12050182

[8] Seok, S., Kim, T., Analytical model for cyclic behavior of cold-formed steel bolted connection frames considering local buckling, Thin-Walled Structures, 207 (2025) 112707, https://doi.org/10.1016/j.tws.2024.112707

[9] Zhou, C., Lang, Z., Huang, S., Dong, Q., Wang, Y., Zheng, W., A comprehensive review of experimental studies on shear behavior of bolted rock joints, Deep Underground Science and Engineering, 1 (2024) 1-21, https://doi.org/10.1002/dug2.12091

[10] Vrtač, T., Kodrič, M., Pogačar, M., Čepon, G., Dynamic substructuring-based identification of the rivet-squeezing force, Mechanical Systems and Signal Processing, 229 (2025) 112487, https://doi.org/10.1016/j.ymssp.2025.112487

[11] Yang, L., Yang, G., Yu, D., Jiang, L., Chen, D., Yuan, Y., Xu, W., Strength characteristics analysis and unified model establishment of bonded, riveted, and adhesive-rivet hybrid CFRP joints, Engineering Structures, 322 (2025) 119121, https://doi.org/10.1016/j.engstruct.2024.119121

[12] Wang, W., Roy, K., Rezaeian, H., Fang, Z., Lim, J. B. P., Moment capacity of cold-formed steel trusses with Howick Rivet Connectors: Tests, modelling and design, Engineering Structures, 322 (2025) 119171, https://doi.org/10.1016/j.engstruct.2024.119171

[13] Tu, X., Liao, Y., Li, B., Li, G., Cui, J., Jiang, H., Design and optimization of rivet structures in the electromagnetic high-speed nailing process, Engineering Optimization, 2025, 1-16, https://doi.org/10.1080/0305215X.2025.2457496

[14] Peng, Y., Yin, J., Wang, X., Chen, X., Wang, K., Huang, Z., Wang, F., Zhang, H., Analysis of the Tensile Mechanical Performance of the Adhesive and Rivet Hybrid Connection in Carbon Fiber Reinforced Composite Rail Vehicles, Composites Communications, 2025, 102347, https://doi.org/10.1016/j.coco.2025.102347

[15] Alsardia, T., Bolt Preload Variations During Repeated Tightening's, Acta Polytechnica Hungarica, 21 (2024) 2

[16] Zabojszcza, P., Radoń, U., Tauzowski, P., Robust Optimization of the Steel Single Story Frame, Acta Polytechnica Hungarica, 21 (2024) 1

[17] Seitl, S. et al., Effects of rivet holes on calibration curves for edge cracks under various loading types in steel bridge structure, 2nd International Conference on Structural Integrity, 2017

[18] Qi, W. et al., Optimization of the Angled Guide Plate for the Vossloh W14-PK Fastener, Acta Polytechnica Hungarica, 19 (2022) 163-182

[19] Grzywiński, M., Weight Optimization of Tower Structures with Continuous Variables using Jaya Algorithm, Acta Polytechnica Hungarica, 21 (2024) 1

[20] Dániel, H., Rad, M. M., Comprehensive Laboratory Test Series for Timber-Concrete Composite Structures, Acta Polytechnica Hungarica, 20 (2023) 1

[21] Ibrahim, S. K., Rad, M. M., Fischer, S., Optimal Elasto-Plastic Analysis of Reinforced Concrete Structures under Residual Plastic Deformation Limitations, Acta Polytechnica Hungarica, 20 (2023) 1

[22] Tanriver, K., Ay, M., Investigation of flue gas temperature effects in natural gas fueled systems: Experimental thermal performance and structural optimization, International Journal of Heat and Fluid Flow, 107 (2024)

[23] Keykha, A. H., The effect of CFRP strengthening on the behavior of deficient steel beams under concentrated and distributed loading, Indian Journal of Engineering & Materials Sciences, 27 (2020) 438-444

[24] Ramasamy, M., et al., Experimental and finite element analysis of titanium based medial tibial condyle using incremental sheet metal forming, Indian Journal of Engineering & Materials Sciences, 28 (2021) 502-508

[25] Sun, H., et al., Quantification Method for Rivet Hole Cracks in an Aircraft Fuselage Using Guided Waves: A BTBD-Theory-Hybrid Space-Time Cross Fusion SpatNet, IEEE Transactions on Industrial Informatics, (2025) https://doi.org/10.1109/TII.2025.3538079

[26] Lin, L., Tong, C., Fu, S., Wu, J., He, W., Zu, L., A prediction of crack propagation on aircraft wing via AK-TCN, Engineering Failure Analysis, 164 (2024) 108693. https://doi.org/10.1016/j.engfailanal.2024.108693

[27] Kim, W., Youn, B. D., Physics-based digital twin updating and twin-based explainable crack identification of mechanical lap joint, Reliability Engineering & System Safety, 253 (2025) 110515, https://doi.org/10.1016/j.ress.2024.110515

[28] Huynh, V. T., Pham, C. H., Pham, V. B., Thai, H. T., Shear strength of beam-end bolted connections in cold-formed steel structures through experiments, numerical simulations and hybrid GPR-ECLPSO modeling, Thin-Walled Structures, 211 (2025) 113114, https://doi.org/10.1016/j.tws.2025.113114

[29] Kang, Y., Kou, S., Meng, K., Zhang, Z., Wang, A., Credal identification of damage patterns in ultra-thin-ply composite bonded/bolted interference-fit joints, Engineering Failure Analysis, 162 (2024) 108371, https://doi.org/10.1016/j.engfailanal.2024.108371

[30] Ihueze, C. C., Okafor, C. E., Omeiza, O. E., Robust Design and Intelligent Modelling of Organic-Based Composites for Armoury Applications, SN Computer Science, 5 (2024) 832, https://doi.org/10.1007/s42979-024-03199-0

[31] Guo, X., et al., Ductile failure of occlusive high strength bolt connections, Journal of Constructional Steel Research, 168 (2020) 1-15, https://doi.org/10.1016/j.jcsr.2020.105982

[32] Ye, J., et al., An improved and robust finite element model for simulation of thin-walled steel bolted connections, Engineering Structures, 250 (2022) 1-25, https://doi.org/10.1016/j.engstruct.2021.113368

[33] Manohar, G., Reddy, V., Vaishali, From fabrication to prediction: Unraveling the tensile strength of Al/SiN composites through machine learning, International Journal of Interactive Design and Manufacturing, (2025) https://doi.org/10.1007/s12008-025-02274-x

[34] Nakahara, T., Hirohata, M., Furuichi, T., An Investigation on Axial Force Reductions of High-strength Bolts by Induction Heating for Paint-coating Removal, Acta Polytechnica Hungarica, 21 (2024) 89-101

[35] Tanriver, K., Ay, M., Topology optimization of a steel construction bolt under boundary conditions, Euroasia Journal of Mathematics, Engineering, Natural & Medical Sciences, 7 (2020) 31-47, https://doi.org/10.1016/j.matdes.2014.06.021

[36] Tanriver, K., Ay, M., Experimental and numerical analysis of bolted two plates using a developed shear theory, Journal of Theoretical and Applied Mechanics, 61 (2023) 509-520

[37] Li, S., et al., Numerical and experimental investigation of fitting tolerance effects on Composite Structures, 115022 (2022)

[38] Tanriver, K., CFD Simulation Analysis of a Diesel Generator Exhaust Muffler and Performance-Based Optimization, Processes, 13 (2025) 887, https://doi.org/10.3390/pr13030887

[39] Nguyen, T. T., et al., Behaviors and design of eccentrically loaded CFST columns with high, Journal of Constructional Steel Research, 188 (2022) 1-16

[40] Ansari, R., Hassani, R., Gholami, Y., Rouhi, H., Numerical nonlinear bending analysis of FG-GPLRC plates with arbitrary shape including cutout, Structural Engineering and Mechanics, 85 (2023) 147-161, https://doi.org/10.12989/sem.2023.85.2.147

[41] Esmaeili, F., Zehsaz, M., Chakherlou, T., Investigation of the effect of tightening torque on the fatigue strength, Materials and Design, 63 (2014) 349-361

[42] Arjomandi, K., Matthews, J., Wyman, B., Flexibility requirement of bolted double-angle shear connections, Journal of Constructional Steel Research (2021)

[43] Hammami, C., Numerical investigation of static behavior of bolted joints, Journal of Theoretical and Applied Mechanics, 60 (2022) 385-394

[44] Pitrakkos, T., et al., Blind bolts with headed anchors under combined tension and shear, Journal of Constructional Steel Research (2021)

[45] Urbas, U., Zorko, D., Vukašinović, N., Machine learning based nominal root stress calculation model for gears with a progressive curved path of contact, Mechanism and Machine Theory, 165 (2021) 104430, https://doi.org/10.1016/j.mechmachtheory.2021.104430

[46] Shahin, R. I., Ahmed, M., Liang, Q. Q., Yehia, S. A., Predicting the web crippling capacity of cold-formed steel lipped channels using hybrid machine learning techniques, Engineering Structures, 309 (2024) 118061, https://doi.org/10.1016/j.engstruct.2024.118061